

## Site-controlled growth of Ge nanostructures on Si(100) via pulsed laser deposition nanostenciling

C. V. Cojocaru

INRS—Énergie, Matériaux et Télécommunications, Université du Québec, 1650 Boul. Lionel-Boulet, Varennes, Québec J3X 1S2, Canada

A. Bernardi, J. S. Reparaz, and M. I. Alonso

Institut de Ciència de Materials de Barcelona-CSIC, Esfera UAB, 08193 Bellaterra, Spain

J. M. MacLeod, C. Harnagea, and F. Rosei<sup>a)</sup>

INRS—Énergie, Matériaux et Télécommunications, Université du Québec, 1650 Boul. Lionel-Boulet, Varennes, Québec J3X 1S2, Canada

(Received 12 July 2007; accepted 20 August 2007; published online 14 September 2007)

The authors combine nanostenciling and pulsed laser deposition to pattern germanium (Ge) nanostructures into desired architectures. They have analyzed the evolution of the Ge morphology with coverage. Following the formation of a wetting layer within each area defined by the stencil's apertures, Ge growth becomes three dimensional and the size and number of Ge nanocrystals evolve with coverage. Micro-Raman spectroscopy shows that the deposits are crystalline and epitaxial. This approach is promising for the parallel patterning of semiconductor nanostructures for optoelectronic applications. © 2007 American Institute of Physics. [DOI: 10.1063/1.2783473]

The growth of germanium (Ge) thin films and structures on silicon (Si) surfaces has been the subject of extensive study due to the prospective device applications<sup>1,2</sup> and the fundamental research importance vis-à-vis the understanding of growth processes.<sup>3–7</sup> In the quest to expand integrated silicon technology, in particular, to applications in optoelectronics, Ge/Si nanoheterostructures<sup>8</sup> with engineered band structures have come under intense investigation as important candidates for light-emitting quantum dot (QD) based devices.

Abundant research efforts have been dedicated to the exploration of “dotlike” structures obtained via the Stranski-Krastanov (SK) growth mode, which comprises the formation of a wetting layer (WL) followed by three-dimensional island (“dot”) formation that relaxes the strain induced by the 4.2% lattice mismatch between Ge and Si. To control the size, shape, and density, but mostly the spatial positioning of Ge dots, many strategies including combinations of lithography-based (top down) and spontaneous self-organization approaches (bottom up) have been pursued.<sup>9–14</sup> Much work has focused on the assisted organization of Ge dots grown on prepatterned Si or SiO<sub>2</sub> substrates either by chemical vapor deposition<sup>15,16</sup> (CVD) or molecular beam epitaxy (MBE).<sup>17–19</sup>

While CVD and MBE have been extensively used, pulsed laser deposition (PLD) emerged just recently<sup>20</sup> as a versatile tool to study the structural<sup>21</sup> and functional<sup>22</sup> properties of self-assembled Ge QDs on silicon substrates. A well-established technique developed mainly to grow high-quality epitaxial films of complex materials,<sup>23</sup> PLD offers additionally the possibility of fine tuning and controlling deposition parameters rather easily in the case of elemental materials. We previously investigated a promising unconventional patterning approach based on direct, selective PLD of functional materials at room temperature through solid-state, reusable nanostencils. This strategy leads to the organization

of nanostructures without any pre patterning or complementary invasive process prior applied to the substrates.<sup>24</sup>

In this letter we describe the patterning of Ge/Si semiconductor heterostructures via PLD nanostenciling at high temperature (600 °C). The intent of this approach is twofold: first, to investigate the kinetic processes of PLD of Ge nanodots and ultimately to compare it with more studied processes such as MBE or CVD, and, second, to demonstrate a flexible approach to gain control over the positioning of ordered arrays of nanostructures with potential applications in device engineering.

To achieve precise positioning of Ge on Si(100), we used nanostencils with hexagonal arrays of circular apertures opened in freestanding, low-stress SiN membranes.<sup>25</sup> These miniature shadow masks were mechanically clamped onto the substrate and the substrate-stencil assembly mounted in front of a rotating Ge solid target (99% purity) [Fig. 1(a)]. Prior to deposition, Si(100) substrates (*n* type, Sb doped resistivity of 0.015 Ω cm) were cleaned in ultrasound solvent baths. The native oxide layer was chemically removed in a 5% HF solution. Ge deposition was performed in high vacuum ( $\sim 10^{-5}$  mbar), using a GSI Lumonics KrF excimer laser ( $\lambda=248$  nm,  $\tau=15.4$  ns) at a repetition rate of 10 Hz and laser fluence on the target of 4 J/cm<sup>2</sup>. The substrate temperature was set at 600 °C and the same stencil was used in consecutive depositions.<sup>26</sup>

Swift fabrication of ordered arrays of Ge structures was achieved in a single deposition step [Fig. 1(b)]. In the initial stages of growth (up to 250 laser ablation pulses) ordered arrays of Ge structures are formed as flat circular mounds, 350 nm in diameter and with a 700 nm periodicity [Fig. 1(c)], i.e., the replica of the design defined by the sieve's apertures. In Fig. 2, scanning electron microscopy (SEM) micrographs for four samples illustrate the patterned Ge islands obtained on Si(100) by varying the number of laser pulses between 250 and 1500 with an estimated rate of  $\sim 0.28$  Å/pulse. SEM micrographs show that with increasing Ge thickness, the shapes of the obtained structures evolve

<sup>a)</sup>Electronic mail: rosei@emt.inrs.ca

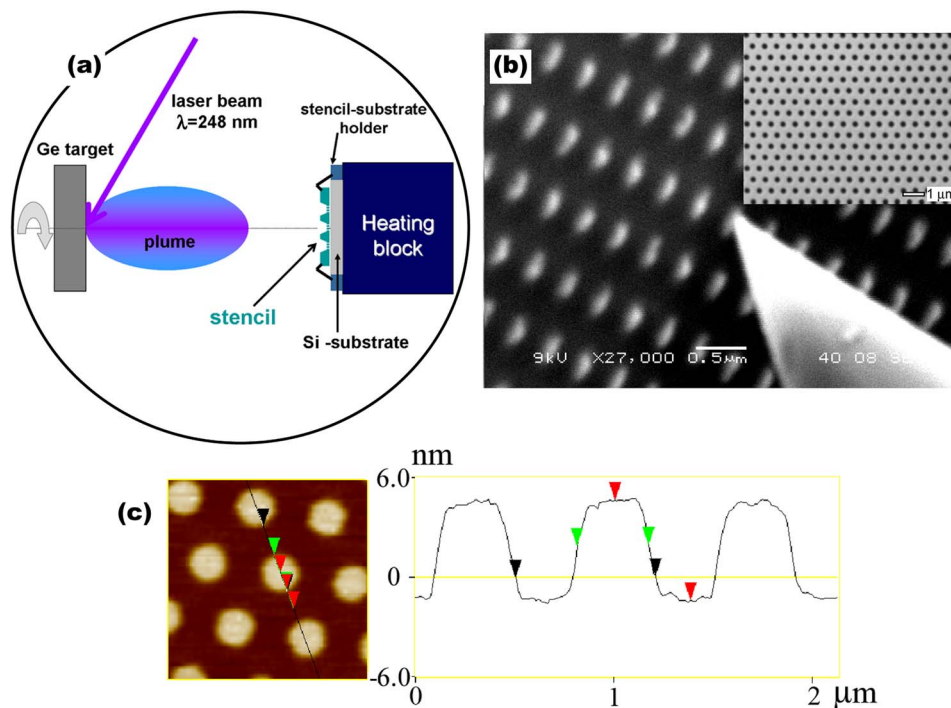


FIG. 1. (Color online) Experimental setup used for stencil deposition and further characterization of Ge ordered arrays: (a) schematic drawing of the PLD-based Ge direct patterning process achieved at high temperature through SiN stencils attached to the Si(100) substrates; (b) SEM micrograph showing an AFM tip scanning across the Ge patterned area in a JEOL-4500 UHV AFM-STM-SEM microscope. The inset shows a detail of a perforated freestanding SiN membrane built in the stencil chip; (c) AFM topography and Ge mound height profile obtained for 250 pulses deposited at 600 °C using a stencil with the architecture shown in the inset (b).

from the flat “two-dimensional (2D)-mound” type [Fig. 2(a)] to three-dimensional (3D) nanocrystalline agglomerations (10–100 nm in lateral size) formed on top of these mounds [Fig. 2(b)], undergoing further a transition to a “coffee-bean-like” grained structure [Fig. 2(c)], and finally coalescing into single nanocrystals [Fig. 2(d)]. Atomic force microscopy (AFM) and SEM images from Figs. 1 and 2 show that all islands are perfectly separated and well defined. The lateral extent of the deposits is always restricted to the range of the aperture areas defined in the stencil.

Micro-Raman spectroscopy was used to provide a structural characterization of the Ge clusters. The optical mea-

surements were carried out by probing the patterned area with the 514.5 nm line of an Ar<sup>+</sup> ion laser focused with a spot size of about 1 μm, i.e., each Raman spectrum (Fig. 3) is collected from the region of two to three apertures. The spectral position and shape of the Ge–Ge phonon mode reveal that the Ge clusters are crystalline, and the absence of the Si–Ge phonon band around ~400 cm<sup>-1</sup> (inset in Fig. 3) clearly indicates that there is no Si intermixing. Further, the Ge–Ge phonon peak becomes more intense with increased

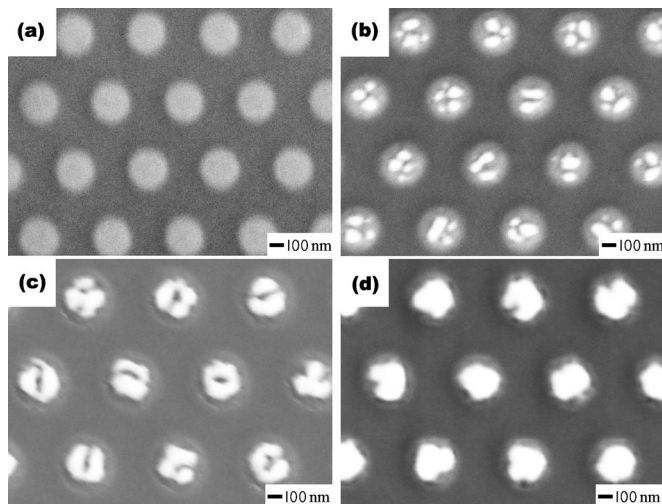


FIG. 2. Coverage dependence of Ge morphology: SEM micrographs showing ordered Ge nanostructures replicated on Si(100) by PLD at 600 °C, for (a) 250, (b) 750, (c) 1250, and (d) 1500 laser pulses with a fluence of 4 J/cm<sup>2</sup>, for a target-substrate distance of 6.5 cm.

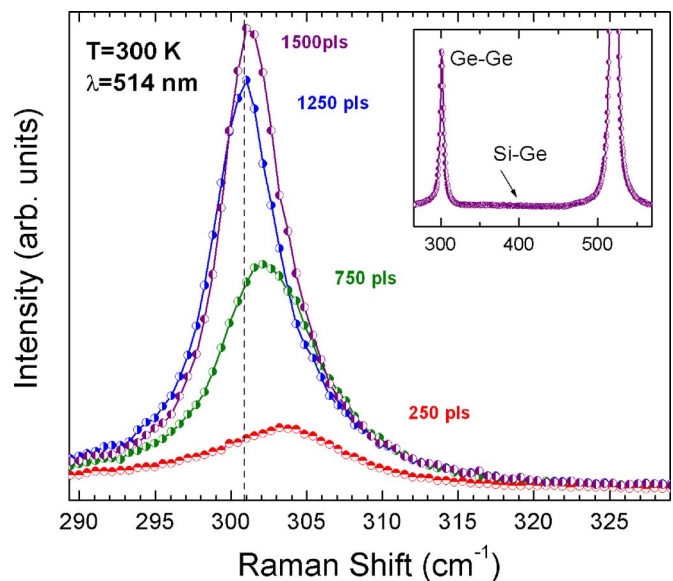


FIG. 3. (Color online) Raman spectra acquired by probing the Ge patterned areas with the 514.5 nm line of an Ar<sup>+</sup> ion laser. The absence of the Si–Ge phonon band around ~400 cm<sup>-1</sup> (see inset) indicates no trace of Si intermixing.

Ge coverage. Spectra recorded after the initial stages of growth exhibit a blueshifted Ge-Ge phonon frequency ( $\sim 303 \text{ cm}^{-1}$ ) attributed to compressive strain ( $\epsilon < -1\%$ ) at the island-substrate interface.<sup>27</sup> The strain is progressively relieved for taller clusters (i.e., higher Ge coverage) whose phonon frequency approaches the value expected for bulk Ge ( $300.8 \text{ cm}^{-1}$ ). The presence of built-in strain suggests that the Ge nanostructures match the Si substrate lattice. In fact, they retain the substrate crystallographic orientation, as confirmed by the phonon selection rules in polarized Raman measurements (not shown here).

The 2D mounds are reminiscent of the thin WL which normally precedes islanding in classical SK growth. AFM topographies indicate that the 2D mounds grow to a maximum height of 6–7 nm, roughly ten times thicker than the critical value for a conventional Ge WL.<sup>28</sup> The anomalous critical thickness for the onset of 3D nucleation can be explained by invoking the finite size of the deposited areas: the 2D mounds, acting as a WL, relieve strain at their periphery, delaying the strain-induced 3D nucleation of structures. Similar phenomenology was discussed in the case of self-assembling of Ge on lithography-patterned windows opened in ultrathin silicon oxide layers.<sup>29</sup>

The dots that initially nucleate on top of the 2D mounds [Fig. 2(b)] are round shaped and their aspect ratios (defined as the dot's height divided by the square root of the base area) range from  $\sim 0.16$  to  $\sim 0.20$ . These dots are reminiscent of the dome-shaped islands observed in Ge/Si(001) heteroepitaxy.<sup>30</sup> The average aspect ratio of the dots increases with coverage to allow for more efficient strain relaxation. Above 500 pulses, we observe a shape transition from rounded to “coffee-bean” dots [Fig. 2(c)]. At this stage of growth, we detect both coalescence of grains and the formation of a depletion region at the center of the underlying 2D mounds, where we expect higher elastic compression. Finally, at higher Ge coverage (above 1000 ablation pulses), the depletion region disappears and is replaced by a single rounded cluster.

The number of Ge dots is of the order of tens per aperture for the samples deposited from 250 up to 500 pulses. For samples deposited up to 1000 pulses, the dots are larger and less numerous [e.g., three to five dots/aperture as shown in Fig. 2(b)]. This implies a feasible control over the number of dots per nominal location and thus their density in the whole patterned area.<sup>31</sup>

In summary, we showed that combining nanostenciling with PLD provides a flexible approach to grow and pattern crystalline Ge/Si nanostructures. The location of the Ge clusters is entirely controlled by the pattern of the nanostencil, and the density and physical dimensions of the dots can be further adjusted by varying the deposition parameters. The morphological evolution of the structures with coverage follows a modified Stranski-Krastanov growth mode due to the finite size of the WL in each aperture location. Raman spectroscopy indicates that the nanostructures are crystalline Ge and that they follow the substrate's crystallographic orientation. In future work we will establish a correlation between the deposition parameters such as laser fluence, substrate orientation and temperature, and the Ge dots' density per deposited site.

The authors acknowledge financial support from the Canada Foundation for Innovation, and NSERC of Canada. F.R. is grateful to FQRNT and the Canada Research Chairs program for salary support. A.B. acknowledges a FPI fellowship. J.S.R. acknowledges financial support from the AlBan fellowship Program. This work was supported in part by the Spanish Ministerio de Educación y Ciencia through Grant No. MAT2006-02680.

- <sup>1</sup>J. Konle, H. Presting, H. Kibbel, K. Thonke, and R. Sauer, *Solid-State Electron.* **45**, 1921 (2001).
- <sup>2</sup>D. L. Hareme, S. J. Koester, G. Freeman, P. Cottrel, K. Rim, G. Dehlinger, D. Ahlgren, J. S. Dunn, D. Greenberg, A. Joseph, F. Anderson, J.-S. Rieh, S. A. S. T. Onge, D. Coolbaugh, V. Ramachandran, J. D. Cressler, and S. Subbanna, *Appl. Surf. Sci.* **224**, 9 (2004).
- <sup>3</sup>D. J. Eaglesham and M. Cerullo, *Phys. Rev. Lett.* **64**, 1943 (1990).
- <sup>4</sup>G. Medeiros-Ribeiro, A. M. Bratkovski, T. I. Kamins, D. A. A. Ohlberg, and R. S. Williams, *Science* **279**, 353 (1998).
- <sup>5</sup>F. M. Ross, J. Tersoff, and R. M. Tromp, *Phys. Rev. Lett.* **80**, 984 (1998).
- <sup>6</sup>J. Stangl, V. Holý, and G. Bauer, *Rev. Mod. Phys.* **76**, 725 (2004).
- <sup>7</sup>F. Ratto, G. Costantini, A. Rastelli, O. G. Schmidt, K. Kern, and F. Rosei, *J. Exp. Nanosci.* **1**, 279 (2006).
- <sup>8</sup>J. M. Baribeau, X. Wu, N. L. Rowell, and D. J. Lockwood, *J. Phys.: Condens. Matter* **18**, R139 (2006).
- <sup>9</sup>J. R. Heath, R. S. Williams, J. J. Shiang, S. J. Wind, J. Chu, C. D'Emic, W. Chen, C. L. Stanis, and J. J. Bucchignano, *J. Phys. Chem.* **100**, 3144 (1996).
- <sup>10</sup>T. I. Kamins and R. S. Williams, *Appl. Phys. Lett.* **71**, 1201 (1997).
- <sup>11</sup>E. S. Kim, N. Usami, and Y. Shiraki, *Appl. Phys. Lett.* **72**, 1617 (1998).
- <sup>12</sup>G. Capellini, M. de Seta, C. Spinella, and F. Evangelisti, *Appl. Phys. Lett.* **82**, 1772 (2003).
- <sup>13</sup>A. Karmous, A. Cuenat, A. Ronda, I. Berbezier, S. Atha, and R. Hull, *Appl. Phys. Lett.* **85**, 6401 (2004).
- <sup>14</sup>A. Bernardi, M. I. Alonso, A. R. Goñi, J. O. Ossó, and M. Garriga, *Appl. Phys. Lett.* **89**, 101921 (2006).
- <sup>15</sup>T. I. Kamins, D. A. A. Ohlberg, R. S. Williams, W. Zhang, and S. Y. Chou, *Appl. Phys. Lett.* **74**, 1773 (1999).
- <sup>16</sup>L. Vescan, *Mater. Sci. Eng., A* **302**, 6 (2001).
- <sup>17</sup>O. G. Schmidt, N. Y. Jin-Phillipp, C. Lange, U. Denker, K. Eberl, R. Schreiner, H. Grabelding, and H. Schweizer, *Appl. Phys. Lett.* **77**, 4139 (2000).
- <sup>18</sup>G. Jin, J. L. Liu, and K. L. Wang, *Appl. Phys. Lett.* **76**, 3591 (2000).
- <sup>19</sup>Z. Zhong, A. Halilovic, M. Muhlberger, F. Schäffler, and G. Bauer, *J. Appl. Phys.* **93**, 6258 (2003).
- <sup>20</sup>B. Shin, J. P. Leonard, J. W. McCamy, and M. J. Aziz, *Appl. Phys. Lett.* **87**, 181916 (2005).
- <sup>21</sup>M. S. Hegazy and H. E. Elsayed-Ali, *J. Appl. Phys.* **99**, 054308 (2006).
- <sup>22</sup>X. Ma, Z. Yan, B. Yuan, and B. Li, *Nanotechnology* **16**, 832 (2005).
- <sup>23</sup>D. B. Chrisey and G. K. Hubler, *Pulsed Laser Deposition of Thin Films* (Wiley, New York, 1994).
- <sup>24</sup>C. V. Cojocaru, C. Harnagea, A. Pignolet, and F. Rosei, *IEEE Trans. Nanotechnol.* **5**, 470 (2006).
- <sup>25</sup>The stencil chip has 14 freestanding membranes, 2 mm in length and 100  $\mu\text{m}$  in width; nominal diameter of the circular apertures is 350 nm and the pitch 700 nm; stencils fabricated at Aquamarijn Filtration, The Netherlands.
- <sup>26</sup>Samples were prepared with various Ge thicknesses (coverages). In PLD, the deposited film thickness is controlled by varying the number of laser pulses for a certain target-substrate distance provided that desorption from the substrate is negligible.
- <sup>27</sup>A. Bernardi, J. O. Ossó, M. I. Alonso, A. R. Goñi, and M. Garriga, *Nanotechnology* **17**, 2602 (2006).
- <sup>28</sup>Typically 0.4–0.6-nm-thick for Ge on Si(001); Y.-W. Mo, D. E. Savage, B. S. Swartzentruber, and M. G. Lagally, *Phys. Rev. Lett.* **65**, 1020 (1990).
- <sup>29</sup>L. Vescan, T. Stoica, B. Holländer, A. Nassiopoulou, A. Olzierski, I. Raptis, and E. Sutter, *Appl. Phys. Lett.* **82**, 3517 (2003).
- <sup>30</sup>A. Rastelli, M. Stoffel, J. Tersoff, G. S. Kar, and O. G. Schmidt, *Phys. Rev. Lett.* **95**, 026103 (2005).
- <sup>31</sup>For any given set of deposition parameters, the sizes of the dots are fairly narrowly distributed. Their density can be further tuned by using stencils with smaller or larger apertures and varying PLD parameters.